Chapter 13

Upconversion Nanomaterials and Its Applications

-Sandeep K. Agarwalla

13.1 Introduction

"Upconversion Materials" (UCM) in general, absorbs two or more photons of lower energy, and emits photons with high energy, featuring large anti-stoke emission maximum up to 560 nm [146]. Upconversion (UC) process is a non-linear optical phenomenon, that converts infrared light into UV/VIS light via sequential absorption & Energy transfer (ET) pathways within Er^{3+}, Ho^{3+} and Tm^{3+} ions. Such items are doped within a suitable host crystal. The UC luminescence (UCL) is greatly controlled/regulated by the host crystal properties like its phase, crystal symmetry, lattice constants, associated crystal field, crystal dimension, chemical nature etc [147, 148]. This parameter is associated with the constituent elements involved and whether host is a binary or ternary system. Again, in order to attain bright UCL, losses via non-radiative processes need to be minimum. It is well known that, the fluoride-based salts are known for low phonon energy relative to oxide-based system. It is known that the upconversion luminescence (UCL) largely depends dopant concentration of activators such as Er^{3+}, Tm^{3+}, Ho^{3+} and sensitizer Yb^{3+} and. The concentration of sensitizer Yb^{3+} plays an important role over upconversion efficiency. Absorption cross-section of Yb^{3+} is relatively large w.r.t. Er^{3+} at given NIR range, that lead to increased UCL. The emitted photons by Yb^{3+} is absorbed by nearby activators Er^{3+} giving rise to UCL. It may be noted that different activators emit in different part of visible spectrum, so but suitable stoichiometric ratio of various activators and sensitizer, upconversion material with tunable colour can be obtained as per requirement.

The few important characteristic properties of UCM are like large anti-stoke emission, high photostability, emission insensitive local environment, almost no auto-fluorescence, no photo-bleaching. Such properties lead UCMs a promising candidate to many important societal applications like:

1) Solar cell efficiency improvement,
2) Bio-probes & Bioimaging & Therapy,
3) Nano-thermometry,

4) Solid state lasers,
5) Lighting,
6) Forensics,
7) Optical fiber based telecommunication etc.

Upconversion materials can act as solar energy harvesters converting unabsorbed IR spectrum into absorbable visible spectrum. Since the excitation wavelength fall in biological window, they can be used for bioimaging and therapy etc.

13.2 Upconversion Process and Characterization

The Upconversion luminescence spectrum from Er^{3+} shows blue (412 nm), green (530 nm and 542 nm) and red (663 nm) emission peaks as shown in the Fig. 13.1 below with absorptions of photons from 980 nm laser. The observed peaks are radiative transitions from

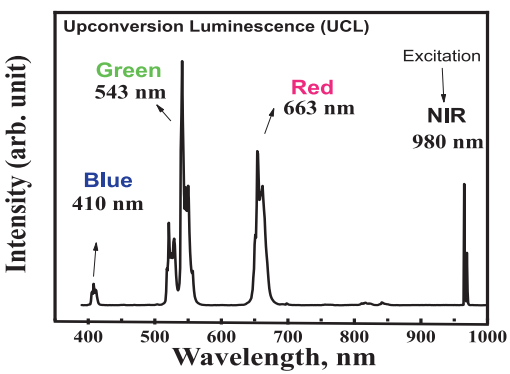

Figure 13.1: The UCL recorded upon signing the Er, Yb co-doped upconversion material. It shows large anti-stoke emission from UCMs.

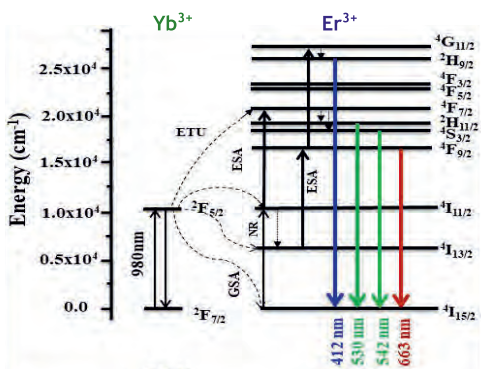

Figure 13.2: Schematic of energy level diagram and various transitions and energy transfer processes for Er^{3+} and Yb^{3+} ions.

$^2H_{9/2} \rightarrow {}^4I_{15/2}$ (blue), $^2H_{11/2} \rightarrow {}^4I_{15/2}$ & $^4S_{3/2} \rightarrow {}^4I_{15/2}$ (green) and $^4F_{9/2} \rightarrow {}^4I_{15/2}$ (red) respectively of Er^{3+} ions in hexagonal $NaYbF_4$ lattice. Both Er^{3+} and Yb^{3+} undergo excitation to higher energy levels through ground state absorption (GSA) by irradiation of 980 nm laser. Subsequent excited state absorption (ESA) from $^4I_{11/2}$ and $^4I_{13/2}$ levels of Er^{3+} and energy transfer upconversion from $^2F_{5/2}$ level of Yb^{3+} to Er^{3+}, followed by non-radiative relaxations (NR), give green and red emissions from Er^{3+} ions present in the sample. Figure 13.2 shows energy level diagram and electronic transitions. The fluorescence intensity of upconverted spectrum depends on incident infra red power by following expression:

$$I = kP^n \tag{13.1}$$

where P is diode laser power and I is the fluorescence intensity at each wavelength and k is the proportionality constant. The value n corresponds the number of photons on a average utilized for generating particular visible wavelength. In order to evaluate the value n for each peak in the spectrum, area under the peak was estimated at various input power and the plot of $\log(I)$ vs. $\log(P)$ was generated. The slope of the plot for each transition was estimated from linear curve fitting method. The value of n is fractional as this upconversion spectrum is not purely two photon or three photon transitions. Also the populations of excited levels of

Er^{3+} ion are populated from sensitizer Yb^{3+} atom through energy transfer (ET) processes. The value of n depends on various mechanisms of excitation and relaxation processes such as ground state absorption, excited state absorption, non radiative relaxation in the host crystal structure, radiative emission and cooperative process of upconversion such as energy transfer from Yb etc. In order to study effect of Bi^{3+}, $NaYbF_4$ and a new host, $NaYb_{1-x}Bi_xF_4$ have been prepared co-doped with Er^{3+} as activator and Yb^{3+} as sensitizer [149]. Their structural and photo-dynamic properties have been investigated in details and results are presented here. The upconversion luminescence at different probe power was recorded and analysed for individual UCL peak in order to find the respective n-value as shown below in Fig. 13.3.

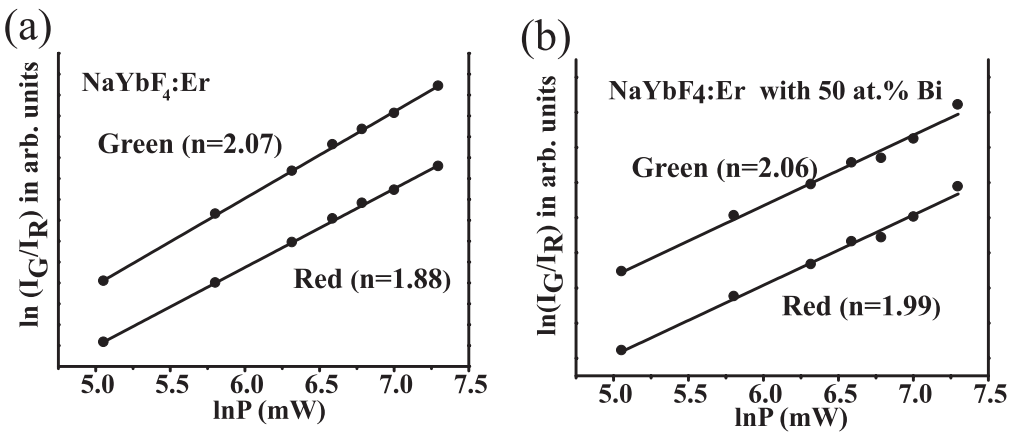

Figure 13.3: Upconversion luminescence intensity Vs laser power for (a) $NaYbF_4$:Er and (b) $NaYbF_4$:Er sample with 50 atom% Bi^{3+} ions.

13.3 Upconversion Material as Thermal Sensor

"$NaYb_{1-x}Bi_xF_4$:Er" was prepared and characterised for developing a "non-contact optical temperature sensor". A non-lanthanide ion namely Bi^{3+} was chosen for replacing Yb^{3+} in $NaYbF_4$ host to investigate its influence on luminescence properties in detail. The typical UCL from Er^{3+} is as shown in Fig. 13.3. The green doublet observed at 530 nm and 542 nm are originating from thermally coupled energy level $^2H_{11/2}$ and $^4S_{3/2}$ respectively with relatively smaller energy gaps. The fluorescence intensity ratio of these two peaks is associated with the temperature of the UCM [150].

Fluorescence intensity ratio (FIR) between the thermally coupled levels $^2H_{11/2}$ and $^4S_{3/2}$ is given by Eq. (13.2):

$$FIR = R = \frac{I_2}{I_1} = \frac{g_2\sigma_2\omega_2}{g_1\sigma_1\omega_1}e^{-\frac{\Delta E}{kT}} \tag{13.2}$$

where g, σ and ω represent respective degeneracy, emission cross-section and angular frequency of levels, $^4S_{3/2}$ (level 1) and $^2H_{11/2}$ (level 2). The terms "k" and "T" represent Boltzmann constant and temperature respectively. The UCL was recorded at various set temperatures as shown in Fig. 13.4. A plot of logarithm of fluorescence intensity ratio (FIR) versus inverse of temperature (1/T) must give a straight line with slope related to ΔE which is energy level difference between the coupled levels 2 and 1 as shown in Fig. 13.5. From the slope ($\Delta E/k$) and fluorescence intensity ratio (FIR) at different temperatures, absolute

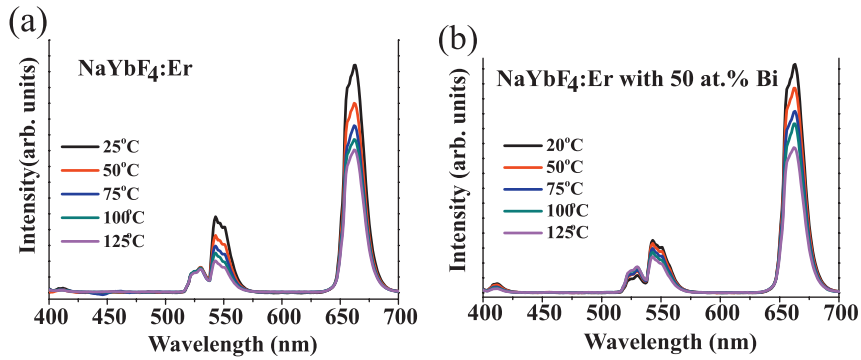

Figure 13.4: Emission spectrum of UPC-NP as a function of temperature for (a) $NaYbF_4$:Er and (b) $NaYbF_4$:Er containing 50 atom% Bi^{3+}. Excitation wavelength was 980 nm.

sensitivity (S) of temperature sensing can be calculated using Eq. (13.3):

$$S = FIR\frac{\Delta E}{k_B T^2} \tag{13.3}$$

For measuring the temperature sensitivity of the developed material, UCL was recorded with sample at various set temperatures as shown in Fig. 13.5. The data analysis based upon the above Eq. (13.3) result the measured sensitivity was reported. The ($NaYb_{1-x}Bi_xF_4$):Er and

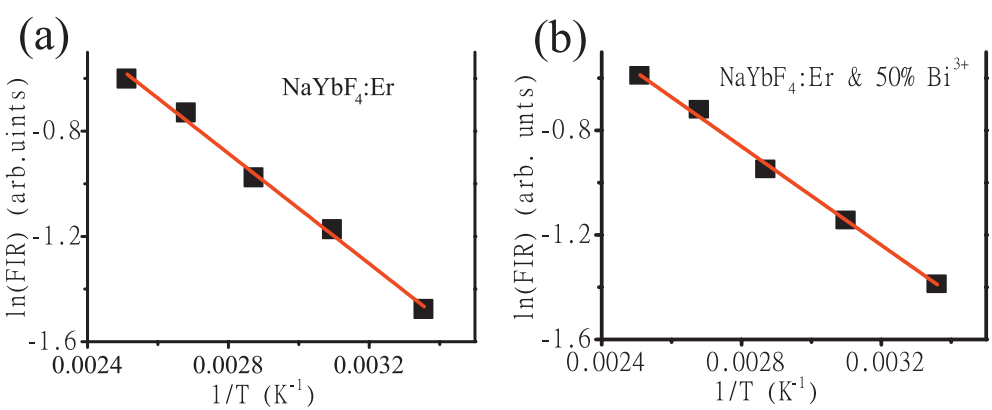

Figure 13.5: Variation of logarithm of FIR as a function of inverse of temperature for (a) $NaYbF_4$:Er and (b) 50 atom% Bi^{3+} in $NaYbF_4$:Er host.

$NaYbF_4$:Er nanoparticles were synthesized using polyol technique and their UCL properties were investigated. Detailed XRD & FTIR studies confirmed partial incorporation of Bi^{3+} in $NaYbF_4$ matrix by replacing Yb^{3+} sites. From steady state photo luminescence and lifetime measurements it is inferred that luminescence intensity from $NaYbF_4$:Er increases with Bi^{3+} addition. The $NaYbF_4$:Er sample containing 50% Bi^{3+} found to be maximum among the various synthesized samples.

13.4 Conclusion

The enhancement in luminescence was based on the increase in Yb^{3+}–Yb^{3+} and Er^{3+}–Er^{3+} distances, reduced extent of dipole–dipole interactions, and the associated decrease in the extent of self-quenching. Energy migration among Yb^{3+} ions in $NaYbF_4$:Er decreased with Bi^{3+} incorporation into the lattice leading to a decrease in the extent of temperature-assisted quenching of luminescence from thermally coupled $^2H_{11/2}$ and $^4S_{3/2}$ levels of Er^{3+}. The new Bi^{3+} incorporated $NaYbF_4$:Er system was also studied towards possible application as an "optical thermometer". The temperature sensitivity of 50% Bi^{3+} containing $NaYbF_4$ sample was found to be $0.0027K^{-1}$ close to other UC material reported in the literature.